GEOPHYSICAL RESEARCH LETTERS, VOL. 37, L06802, doi:10.1029/2009GL042313, 2010

Sheared deep vortical convection in pre-depression Hagupit during TCS08

Michael M. Bell[1,2] and Michael T. Montgomery[1,3]

Received 28 December 2009; accepted 4 February 2010; published 17 March 2010.

[1] Airborne Doppler radar observations from the recent Tropical Cyclone Structure 2008 field campaign in the western North Pacific reveal the presence of deep, buoyant and vortical convective features within a vertically-sheared, westward-moving pre-depression disturbance that later developed into Typhoon Hagupit. On two consecutive days, the observations document tilted, vertically coherent precipitation, vorticity, and updraft structures in response to the complex shearing flows impinging on and occurring within the disturbance near 18 north latitude. The observations and analyses herein suggest that the low-level circulation of the pre-depression disturbance was enhanced by the coupling of the low-level vorticity and convergence in these deep convective structures on the meso-gamma scale, consistent with recent idealized studies using cloud-representing numerical weather prediction models. Further examination of these new observations is needed to quantify the relative role of these vortical convection features in the tropical cyclone spin up process. **Citation:** Bell, M. M., and M. T. Montgomery (2010), Sheared deep vortical convection in pre-depression Hagupit during TCS08, *Geophys. Res. Lett.*, *37*, L06802, doi:10.1029/2009GL042313.

1. Introduction

[2] A recent meteorological field experiment sponsored by the U. S. Office of Naval Research, entitled Tropical Cyclone Structure 2008 (TCS08), was conducted during August and September 2008. One of the scientific objectives of TCS08 was to further understand and improve the prediction of the formation of typhoons in the western north Pacific (WPAC) sector [*Elsberry and Harr*, 2008].

[3] In a recent observational survey spanning four consecutive years during the peak of the hurricane season in the tropical Atlantic and eastern Pacific basins, *Dunkerton et al.* [2009] suggested that tropical cyclones in the deep tropics develop from a lower tropospheric, cyclonic "Kelvin's cat's eye" circulation within an easterly wave critical layer located equatorward of the easterly jet axis that typifies the trade wind belt. It was not until very recently that this tropical cyclogenesis sequence was tested with real data in the WPAC. *Montgomery et al.* [2009a] examined the synoptic and subsynoptic scale aspects of the formation of Typhoon Nuri (2008) that occurred during the TCS08 experiment, and suggested that the pre-Nuri disturbance was of the easterly wave type with the preferred location for storm genesis near the center of the cat's eye recirculation region that was readily apparent in the frame of reference moving with the wave disturbance. This work suggests that this new cyclogenesis model is applicable in easterly flow regimes and can prove useful for tropical weather forecasting in the WPAC. It reaffirms also that easterly waves or other westward propagating disturbances are often important ingredients in the formation process of typhoons [*Chang*, 1970; *Reed and Recker*, 1971; *Ritchie and Holland*, 1999]. Although the Nuri study offers compelling support for the large-scale ingredients of this new tropical cyclogenesis model [*Dunkerton et al.*, 2009], it leaves open important unanswered questions about the convective-scale processes that operate within the cat's eye recirculation region.

[4] The westward moving disturbance that eventually became Typhoon Hagupit (2008) during the TCS08 field experiment offers an opportunity to study convective (meso-gamma, 2–20 km) scale aspects of the genesis sequence within an identifiable recirculation region several days prior to the declaration of a tropical depression by the Joint Typhoon Warning Center. The purpose of this paper is to begin to clarify the meso-gamma scale processes that are thought to have contributed to the formation of the incipient Typhoon Hagupit by employing new observations of convective structures within a protected recirculation region.

2. Synoptic Overview of Pre-depression Hagupit

[5] The precursor disturbance that eventually became Typhoon Hagupit was initially identifiable in infrared satellite imagery as a convective burst on 8 September near 180 E longitude (Figure 1a). No clear wave structure or significant vorticity maximum were apparent in the low-level flow in the GFS FNL analysis fields, but satellite estimates of total precipitable water were 10–20 mm higher than in the surrounding region (not shown). An 850 hPa relative vorticity maximum exceeding 2×10^{-5} s^{-1} (cyan overlay in Figure 1) was apparent in the GFS analysis around 0000 UTC 9 September the following day (Figure 1b) as the convective area moved westward. The red line in Figure 1 indicates the approximate 4 m s^{-1} westward translation of both the convection and 850 hPa vorticity anomaly that gradually increased in amplitude over time (Figures 1a–1h). The location of the disturbance at 18 N latitude is located well north of the intertropical convergence zone, and significantly east of any southwesterly monsoonal flow. The low-level vorticity maximum, enhanced humidity, and westward propagation speed are broadly consistent with the composite structure of western Pacific easterly waves described by *Lau and Lau* [1990].

[1]Department of Meteorology, Naval Postgraduate School, Monterey, California, USA.
[2]National Center for Atmospheric Research, Boulder, Colorado, USA.
[3]Hurricane Research Division, AOML, NOAA, Miami, Florida, USA.

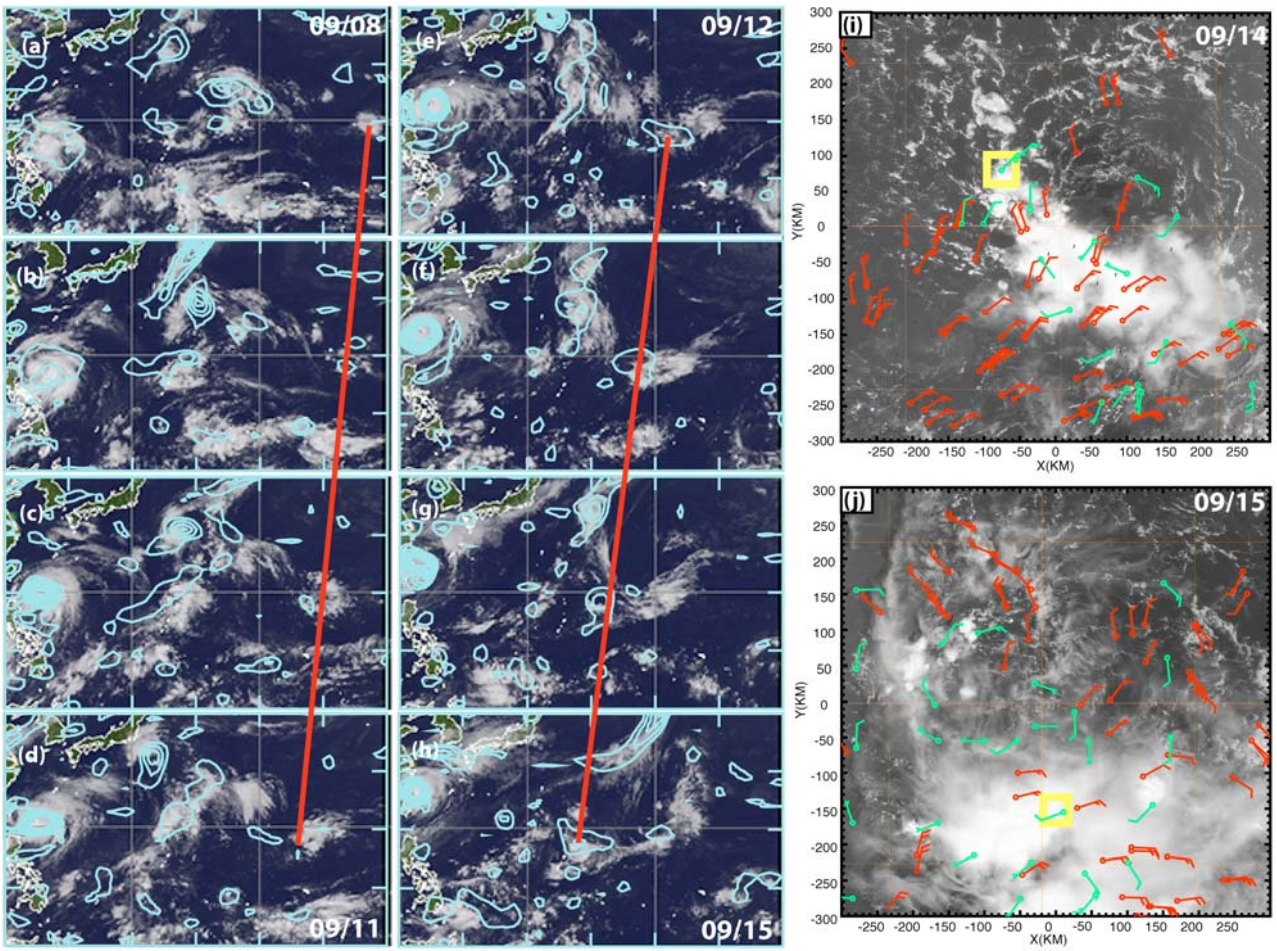

Figure 1. (a–h) MTSAT IR imagery at 0030 UTC from 8–15 September and 850 hPa relative vorticity from the GFS FNL analysis. Domain is from 0–40 N latitude and 120–180 E longitude. The red line follows the convective activity associated with the pre-Hagupit disturbance as it moves westward. Cyan vorticity contours are every 4×10^{-5} s^{-1} with a minimum contour value of 2×10^{-5} s^{-1}. (i and j) Satellite and dropwindsonde composites centered at 18 N and 150 (Figure 1i) and 148 (Figure 1j) E on 14 and 15 September. Green wind barbs indicate surface (10 m altitude) winds from dropwindsondes released during the research flights. Red wind barbs indicate atmospheric motion vectors in the 150–250 hPa layer at 0057 UTC (Figure 1i) and 2057 UTC (Figure 1j) overlaid on visible satellite imagery from the Terra MODIS satellite at 0030 UTC 14 Sep. (Figure 1i) and 0113 UTC 15 Sep. (Figure 1j). Yellow boxes indicate aircraft radar analysis locations in Figures 2 and 3.

[6] As the disturbance moved into the TCS08 research domain, the first of two missions was flown by the Naval Research Lab P-3 aircraft (NRL P3) with the NCAR Electra Doppler Radar (ELDORA) around ~0000 UTC 14 September 2008. At this time, pre-Hagupit was southwest of an upper-tropospheric trough that was evident as a large cyclonically-curved band of cloud tops in the infrared imagery (Figure 1g). Upper-level northwesterlies associated with the trough are evident in 150–250 hPa layer atmospheric motion vectors (red wind barbs in Figure 1i) derived from consecutive satellite images [*Velden et al.*, 2005]. Dropwindsondes released by the NRL P3 revealed a weak, closed low-level circulation (LLC) at the surface (green wind barbs in Figure 1i), setting up a deep layer northwesterly shear exceeding 10 m s^{-1} over the loosely organized convection evident in visible satellite imagery (background in Figure 1i). The LLC was persistent 24 hours later during the next mission that included dropsondes from the U.S. Air Force WC130-J aircraft as the disturbance moved west of the trough into a region with reduced deep layer shear (Figure 1j). These two research missions occurred four and three days, respectively, prior to the declaration of this storm as a tropical depression by the Joint Typhoon Warning Center at 1800 UTC 18 September. The tropical cyclone went on to intensify into a 125 kt typhoon in the South China Sea and cause damage in several countries with at least 67 deaths and an estimated 1 billion U.S. dollars in property damage.

3. Mesoscale Radar Observations

[7] ELDORA radar analysis from pre-Depression Hagupit during TCS08 indicates vorticity-rich, buoyant convective plumes (aka Vortical Hot Towers or VHTs) near the developing low-level circulation consistent with the "bottom-up" pathway of tropical cyclogenesis [*Montgomery and Enagonio*, 1998; *Tory and Montgomery*, 2006; *Montgomery et al.*, 2006]. The ELDORA data were first corrected for navigation errors and edited to remove the ocean surface echoes,

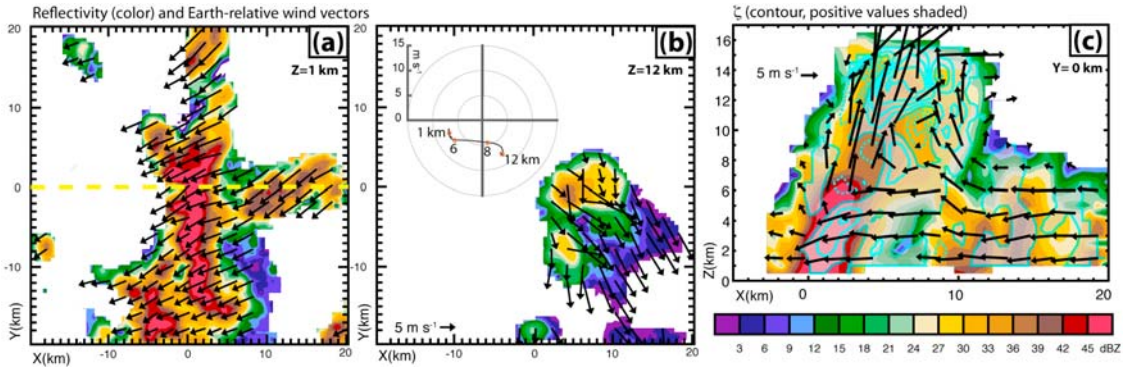

Figure 2. ELDORA analysis from 0036–0058 UTC 14 September, 2008. Horizontal plan view of radar reflectivity (color, dBZ) and wind vectors are shown at (a) 1 km and (b) 12 km altitude. (c) Reflectivity (color), relative vertical vorticity (4×10^{-3} s^{-1} contours, positive [cyclonic] values shaded), and wind vectors in the X–Z plane. Yellow dashed line in Figure 2a depicts the vertical cross-section in Figure 2c. Inset in Figure 2b is radar-derived velocity hodograph.

noise, and other radar artifacts [*Oye et al.*, 1995; *Bosart et al.*, 2002]. Then, the three-dimensional dual-Doppler winds, precipitation, and perturbation temperature and buoyancy fields were obtained on an isotropic 500 m grid by variational techniques [*Roux et al.*, 1993; *Reasor et al.*, 2009; *Houze et al.*, 2009]. These three-dimensional airborne radar observations are unique in both their location in the western Pacific basin, and in the high-resolution structure of convective elements at the meso-gamma scale early in the life cycle of a tropical cyclone.

[8] Analysis of ELDORA data from the boxed region in Figure 1i indicates a quasi-linear organization of shallow and deep convection (Figure 2) near the center of the LLC. Earth-relative winds at 1 km altitude (~900 hPa) indicate northeasterly flow on the northwestern side of the LLC (vectors). Reflectivity exceeding 40 dBZ at 12 km height exists in the deepest convection along the line displaced to the east of the low-level reflectivity maximum (Figure 2b), with a shifting of the winds to stronger northwesterlies aloft. The hodograph (inset in Figure 2b) derived by averaging the radar winds at each level in the 1600 km^2 domain has counterclockwise turning of the winds with height and an ~11 m s^{-1} northwesterly shear vector from 850–200 hPa that is consistent with the satellite wind estimates.

[9] A vertical east-west cross-section through the deep, tilted structure in Figure 2c indicates strong convergence of the low- and mid-level easterly flow at the leading edge of the convective line and an intense, tilted updraft with a maximum vertical velocity of ~25 m s^{-1} at 12 km altitude. This convective structure has a strong, low-level, positive vertical vorticity core up to 6 km altitude (shaded region) that is tilted also, with peak values exceeding 8×10^{-3} s^{-1} at 4 km altitude. At 1 km altitude, the 4×10^{-3} s^{-1} vorticity is ~100 times greater than the planetary vorticity at this latitude, and an order of magnitude larger than the pre-existing, low-level, cyclonic vorticity on the meso-beta scale (20 – 200 km) independently calculated to be ~2×10^{-4} s^{-1} (not shown). In the middle and upper-troposphere the vorticity structure consists of multiple dipoles, with a maximum positive value of ~20×10^{-3} s^{-1} aloft. To understand the origin of these intense vorticity dipoles it is necessary to recall the three-dimensional vorticity equation for a rotating fluid and the specific contributions to the vertical vorticity arising from tilting and stretching of horizontal and vertical vortex lines, respectively [e.g., *Pedlosky*, 1979, equation (2.4.6)]. Upon calculating the horizontal vorticity from the analyzed wind field (not shown), we find that the upper-level vertical vorticity maximum (and accompanying negative minimum) is consistent with the tilting of horizontal vorticity associated primarily with the horizontal shear of the updraft. Similarly, the vorticity dipoles apparent in the mid-troposphere are found to be consistent with the tilting of horizontal vorticity, with a larger contribution coming from the vertical shear of the horizontal wind.

[10] The tilted vortex structure revealed in the ELDORA observations is more complex than previously documented VHT structures in idealized numerical simulations that only possess vertical shear associated with a warm-core vortex [*Montgomery et al.*, 2006; *Nguyen et al.*, 2008]. The significance of these ELDORA observations is that they confirm the existence of vortical, deep convective structures in the tropics even in a realistic vertically sheared environment rich in vertical vorticity on the meso-beta scale. The co-location of strong vertical vorticity and convergence in the *lower troposphere* implicates stretching of the pre-existing low-level cyclonic vorticity, consistent with the 'VHT amplification pathway' in idealized numerical simulations.

[11] When the NRL P3 surveyed the pre-depression ~24 hours later, the mid-to-upper tropospheric flow had shifted to the northeast and the deep tropospheric vertical shear over the system had decreased. However, ELDORA observations indicate that a complex mesoscale vertical shear pattern was still affecting the deep convection that continued to erupt within the disturbance. The dual-Doppler reflectivity and ground-relative horizontal winds at 1, 2.5, and 6 km heights indicate a VHT-like structure on the southeastern side of the LLC at ~2355 UTC 14 September (Figures 3a–3c). Southwesterly flow associated with the weak, ground-relative, meso-*beta* scale, closed cyclonic circulation at 1 km is indicated in Figure 3a, with a local closed circulation at the meso-*gamma* scale at 2.5 km altitude depicted in Figure 3b. At 6 km altitude (Figure 3c), a stronger flow from the northeast is evident through the convective core. The radar-derived hodograph exhibits a strong northeasterly shearing flow in the lower troposphere, with a mid-level maximum at the 6 km (~500 mb) level, but weaker winds aloft. Vertical cross-sections through the deep

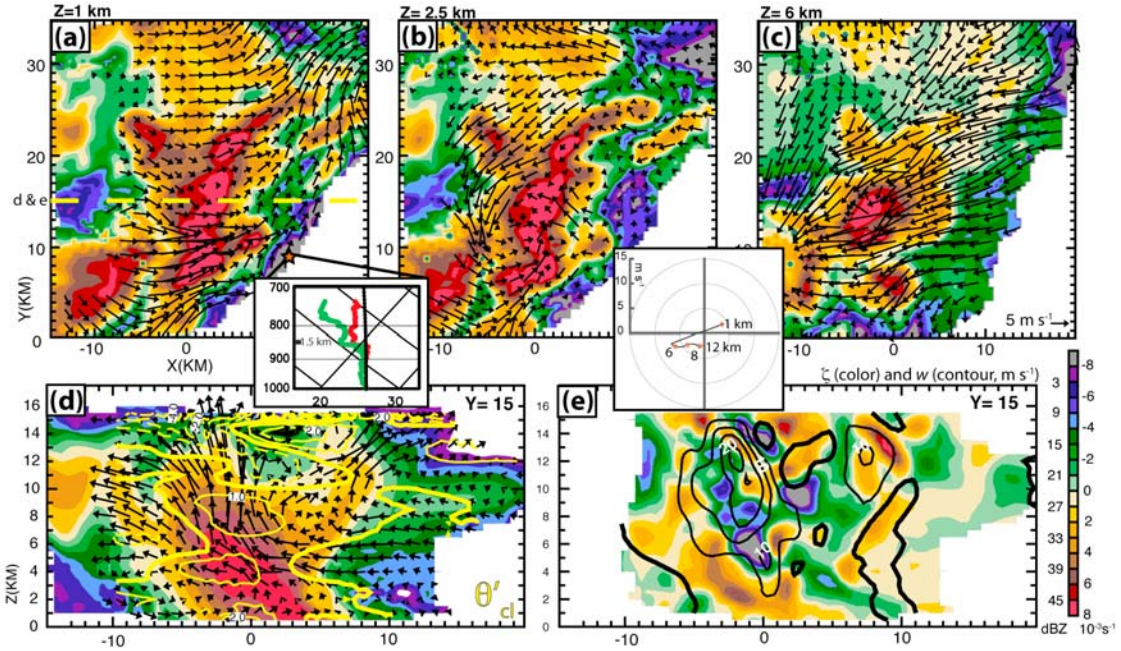

Figure 3. ELDORA analysis from 2351–2358 UTC 14 September, 2008. (a–c) Horizontal plan view of radar reflectivity (color, dBZ), and wind vectors in the earth-relative frame at 1, 2.5, and 6 km altitude. (d) Reflectivity (color), wind vectors in the X–Z plane, and yellow contours indicate 1 K temperature perturbations (solid positive, dashed negative). (e) Relative vertical vorticity (color, 10^{-3} s^{-1}) and vertical velocity (contour, m s^{-1}).The yellow dashed line in Figure 3a depicts the location of the vertical slice in Figures 3d and 3e, and the orange star marks the location of the thermodynamical sounding shown in the left inset. Right inset shows radar-derived velocity hodograph.

convection (Figures 3d and 3e) reveal a similar structure as on the previous day, with reflectivity values reaching 16 km altitude, but with an oppositely tilted direction. The southwest tilt of the convection with height is consistent with the change in direction and magnitude of the mid-level shear and reduction in upper-level winds (the tower is less tilted in the upper troposphere than on the previous day). The entire updraft is nearly 15 km wide (vectors in panel d, magnitude contoured in panel e) and has a two-pronged structure above 10 km height with a nearly vertical branch exceeding 20 m s^{-1} and a weaker up-shear branch of 10 m s^{-1} separated by a weak downdraft region. While the exact magnitude of the vertical motion is dependent on the radar editing, geometry, and analysis technique, the overall structure of the updraft is similar in breadth and magnitude to the independent analysis on the previous day, and is similar also to the massive convective updraft in Tropical Depression Ophelia documented by *Houze et al.* [2009].

[12] A pressure and buoyancy retrieval reveals a weak pressure perturbation associated with the low-level mesocyclone (not shown), but suggests that the primary force responsible for the strong vertical motion is cloud buoyancy, with a local warm anomaly of ~1 K (yellow contour in panel d) co-located with the convective core. This retrieval is consistent with the thermodynamic profile (top-left inset in Figure 3) obtained from a dropsonde released near the orange star in panel (a), that indicates a nearly saturated layer below 1.5 km where lifted parcels would condense, release latent heat, and become buoyant relative to the surrounding environment. The vorticity structure (Figure 3e) is similar to the tower in Figure 2c, with a substantial positive region below 2 km and a peak lower-tropospheric value near 6×10^{-3} s^{-1}. Strong vorticity dipoles are evident in the middle and upper troposphere. These dipoles are consistent with tilting of horizontal vorticity associated primarily with the vertical shear of the horizontal wind in the middle troposphere, and with horizontal shear of the updraft in the upper troposphere, similar to the previous day (Figure 2c).

4. Summary and Conclusions

[13] The ELDORA radar analysis from pre-depression Hagupit in the western North Pacific offers an unprecedented look at the structure of deep vortical convection in the tropics under the influence of vertical wind shear associated with the ambient and local environmental flow. In some respects, the overall structure of these deep, buoyant, and vortical convective features resemble the VHTs documented in recent idealized numerical simulations of tropical cyclone spin-up [*Montgomery et al.*, 2006; *Nguyen et al.*, 2008]. However, their structure is more complex because of the non-negligible, environmental vertical shearing flow that tends to tilt the updrafts, contribute additional sources of horizontal vorticity that can be tilted into the vertical, and organize the convection as part of mesoscale linear features [*LeMone et al.*, 1998]. This linear organization is similar to the convective structures observed in previous analyses of tropical depressions [*Zipser and Gautier*, 1978; *Reasor et al.*, 2005; *Houze et al.*, 2009].

[14] Although the vertical wind shear changed significantly between the two analysis days, and varied also across the disturbance, a consistent juxtaposition of tilted precipitation, vertical vorticity, and updraft columns was apparent. The corroboration of these vortical convective structures

within a recirculation region at 18 N latitude, even in the presence of a complex vertically shearing flow, is consistent with the basic tenet that the pre-existing low-level circulation is enhanced by the coupling of the low-level vorticity and convergence in deep convection on the meso-gamma scale. On the basis of these observations, together with recent idealized numerical modeling studies demonstrating that these convective structures serve as the building blocks for the tropical depression vortex [*Nguyen et al.*, 2008; *Montgomery et al.*, 2009b], we hypothesize that repeated convective bursts similar to those documented here were primarily responsible for the formation of Hagupit as the disturbance moved westward in the western North Pacific.

[15] Continued analysis of these observations and testing of this hypothesis is currently underway by TCS08 science team members. Planned work includes an examination of the spectrum of convection in pre-depression Hagupit (2008) and pre-typhoon Nuri (2008), merger of remnant meso-gamma scale convective vortices, diabatically-induced convergence and frictional influences on the storm scale, and their net impact on the system-scale circulation at the meso-beta scales (D. Raymond, personal communication, 2009; L. Lussier, personal communication, 2009).

[16] **Acknowledgments.** The authors would like to acknowledge all of the TCS08 participants for their efforts in collecting the dataset used in this study, and especially Pat Harr for his leadership in executing the field program successfully. Reviews provided by Peter Black, Russell Elsberry, Wen-Chau Lee, Michael Riemer, Roger Smith, and an anonymous reviewer helped improve the manuscript. Research was supported by grant N001408WR20129 from the U.S. Office of Naval Research, NSF grants ATM-0733380, ATM-0715426, ATM-0649944 and the U.S. Naval Postgraduate School in Monterey, CA.

References

Bosart, B. L., W.-C. Lee, and R. M. Wakimoto (2002), Procedures to improve the accuracy of airborne Doppler radar data, *J. Atmos. Oceanic Technol.*, *19*, 322–339.

Chang, C. P. (1970), Westward propagating cloud patterns in the tropical Pacific as seen from time-composite satellite photographs, *J. Atmos. Sci.*, *27*, 133–138, doi:10.1175/1520-0469(1970)027<0133:WPCPIT>2.0.CO;2.

Dunkerton, T. J., M. T. Montgomery, and Z. Wang (2009), Tropical cyclogenesis in a tropical wave critical layer: Easterly waves, *Atmos. Chem. Phys.*, *9*, 5587–5646.

Elsberry, R. L., and P. A. Harr (2008), Tropical cyclone structure (TCS08) field experiment science basis, observational platforms, and strategy, *Asia Pac. J. Atmos. Sci.*, *44*, 209–231.

Houze, R. A., W.-C. Lee, and M. M. Bell (2009), Convective contribution to the genesis of Hurricane Ophelia (2005), *Mon. Weather Rev.*, *137*, 2778–2800, doi:10.1175/2009MWR2727.1.

Lau, K.-H., and N.-C. Lau (1990), Observed structure and propagation characteristics of tropical summertime synoptic scale disturbances, *Mon. Weather Rev.*, *118*, 1888–1913, doi:10.1175/1520-0493(1990)118<1888:OSAPCO>2.0.CO;2.

LeMone, M. A., E. J. Zipser, and S. B. Trier (1998), The role of environmental shear and thermodynamic conditions in determining the structure and evolution of mesoscale convective systems during TOGA COARE, *J. Atmos. Sci.*, *55*, 3493–3518, doi:10.1175/1520-0469(1998)055<3493:TROESA>2.0.CO;2.

Montgomery, M. T., and J. Enagonio (1998), Tropical cyclogenesis via convectively forced vortex Rossby waves in a three-dimensional quasi-geostrophic model, *J. Atmos. Sci.*, *55*, 3176–3207, doi:10.1175/1520-0469(1998)055<3176:TCVCFV>2.0.CO;2.

Montgomery, M. T., M. E. Nicholls, T. A. Cram, and A. B. Saunders (2006), A vortical hot tower route to tropical cyclogenesis, *J. Atmos. Sci.*, *63*, 355–386, doi:10.1175/JAS3604.1.

Montgomery, M. T., L. L. Lussier III, R. W. Moore, and Z. Wang (2009a), The genesis of Typhoon Nuri as observed during the tropical cyclone structure 2008 (TCS-08) field experiment—Part 1: The role of the easterly wave critical layer, *Atmos. Chem. Phys. Discuss.*, *9*, 19,159–19,203.

Montgomery, M. T., Z. Wang, and T. J. Dunkerton (2009b), Intermediate and high resolution numerical simulations of the transition of a tropical wave critical layer to a tropical storm, *Atmos. Chem. Phys. Discuss.*, *9*, 26,143–26,197.

Nguyen, V. S., R. Smith, and M. T. Montgomery (2008), Tropical cyclone intensification and predictability in three dimensions, *Q. J. R. Meteorol. Soc.*, *134*, 563–582, doi:10.1002/qj.235.

Oye, R., C. Mueller, and S. Smith (1995), Software for radar translation, visualization, editing, and interpolation, paper presented at 27th Conference on Radar Meteorology, pp. 359–361, Am. Meteorol. Soc., Vail, Colo.

Pedlosky, J. (1979), *Geophysical Fluid Dynamics*, 624 pp., Springer, New York.

Reasor, P. D., M. T. Montgomery, and L. F. Bosart (2005), Mesoscale observations of the genesis of Hurricane Dolly (1996), *J. Atmos. Sci.*, *62*, 3151–3171, doi:10.1175/JAS3540.1.

Reasor, P. D., M. D. Eastin, and J. F. Gamache (2009), Rapidly intensifying Hurricane Guillermo (1997). Part I: Low-wavenumber structure and evolution, *Mon. Weather Rev.*, *137*, 603–631, doi:10.1175/2008MWR2487.1.

Reed, R. J., and E. E. Recker (1971), Structure and properties of synoptic-scale wave disturbances in the equatorial western Pacific, *J. Atmos. Sci.*, *28*, 1117–1133, doi:10.1175/1520-0469(1971)028<1117:SAPOSS>2.0.CO;2.

Ritchie, E. A., and G. J. Holland (1999), Large-scale patterns associated with tropical cyclogenesis in the western Pacific, *Mon. Weather Rev.*, *127*, 2027–2043, doi:10.1175/1520-0493(1999)127<2027:LSPAWT>2.0.CO;2.

Roux, F., V. Marécal, and D. Hauser (1993), The 12/13 January 1988 narrow cold-frontal rainband observed during MFDP/FRONTS 87. Part I: Kinematics and thermodynamics, *J. Atmos. Sci.*, *50*, 951–974, doi:10.1175/1520-0469(1993)050<0951:TJNCFR>2.0.CO;2.

Tory, K. J., and M. T. Montgomery (2006), Internal influences on tropical cyclone formation, paper presented at Sixth International Workshop on Tropical Cyclones, World Meteorol. Soc., San Jose, Costa Rica.

Velden, C., et al. (2005), Recent innovations in deriving tropospheric winds from meteorological satellites, *Bull. Am. Meteorol. Soc.*, *86*, 205–223, doi:10.1175/BAMS-86-2-205.

Zipser, E. J., and C. Gautier (1978), Mesoscale events within a GATE tropical depression, *Mon. Weather Rev.*, *106*, 789–805, doi:10.1175/1520-0493(1978)106<0789:MEWAGT>2.0.CO;2.

M. M. Bell and M. T. Montgomery, Department of Meteorology, Naval Postgraduate School, 589 Dyer Rd., Monterey, CA 93943-5114, USA. (mmbell@nps.edu)